Available online at www.sciencedirect.com
SCIENCE DIRECT®
International Journal of Heat and Mass Transfer 47 (2004) 385–393
International Journal of HEAT and MASS TRANSFER
www.elsevier.com/locate/ijhmt

Prediction of friction factors and heat transfer coefficients for turbulent flow in corrugated tubes combined with twisted tape inserts. Part 2: heat transfer coefficients

Ventsislav Zimparov *

Gabrovo Technical University, 4 Hadji Dimitar Street, BG-5300 Gabrovo, Bulgaria

Received 5 February 2003

Abstract

A simple mathematical model following the suggestion of Smithberg and Landis has been created to predict the heat transfer coefficients for the case of a fully developed turbulent flow in a spirally corrugated tube combined with a twisted tape insert. The heat transfer can be predicted from the combined effects of the axial and the tangential boundary layer flows coupled with an additional ''vortex mixing'' effect near the wall through the solution of the corresponding momentun and energy transfer equations. The ''wall roughness'' has an effect simultaneously on the axial velocity, secondary fluid motion and the resulting swirl mixing. The model reflects the influence of the ''wall roughness'' and the twisted tape on the thermal resistances of the helicoidal core flow, twisting boundary layer flow and the viscous sublayer near the wall. The calculated heat transfer coefficients have been compared to 544 experimental points obtained from 57 tubes tested. Four hundred thirty-eight points (80.5%) have a relative difference of less than ±15% and 106 points (19.5%) have a relative difference between ±(15–20)%.

Keywords: Compound heat transfer; Corrugated tubes with twisted tape inserts; Heat transfer coefficient; Single-phase turbulent flow

1. Introduction

It has been well known for many years that the performance of heat exchangers, for single-phase flows in particular, can be substantially improved by many augmentation techniques [1]. They are classified into passive and active techniques. The former use surface modification or an additional device incorporated into the channel. Typical examples of passive augmentation techniques are surface roughness, displaced promoters and vortex generators. Surface roughness has been used to reduce the thickness of the boundary layer close to the surface and to introduce better fluid mixing. Displaced promoters include inserts that alter the flow mechanism near the surface by disturbing the core flow. A vortex flow can be created through coiled wires, stationary propellers or twisted tapes.

Twisted tape inserts as passive enhancement devices have been used for almost a century. After their early application in the flue-ways of tube-fire boilers, today the focus of energy conservation has generated renewed interest in the use of twisted tape inserts. It is important to note that the wall roughness elements influence the flow pattern only across a relatively thin fluid layer close to the wall of the tube. In contrast to small roughness elements and ribs, the twisted tape inserts cause alteration in the entire flow pattern creating rotating and/or secondary flows [2]. In general the heat transfer enhancement is attributed to several mechanisms: increased flow path length, increased flow velocity/reduced hydraulic diameter, tape-generated swirl motion and tape fin effects. The fin effects are shown to be less significant for a snug to loose fitting twisted tapes [3,4]. Geometrically a twisted tape insert is characterized by

* Fax: +359-66-801155.
E-mail address: vdzim@tugab.bg (V. Zimparov).

0017-9310/$ - see front matter © 2003 Elsevier Ltd. All rights reserved.
doi:10.1016/j.ijheatmasstransfer.2003.08.004

Nomenclature

A	surface area (m^2)
D	tube diameter (m)
e	ridge height (m)
H	pitch of the twisted tape (m)
L	length of the tube (m)
l	mixing length (m)
$\dot{m}$	mass flow rate ($kg\,s^{-1}$)
p	pitch of ridging (m)
Δp	pressure drop (Pa)
r_0	tube radius (m)
U	axial velocity component ($m\,s^{-1}$)
u_*	shear velocity $(\tau_w/\rho)^{1/2}$ ($m\,s^{-1}$)
V	total velocity vector ($m\,s^{-1}$)
y	distance from the wall (m)

Greek symbols

β	helix angle of rib (°)
δ	thickness of the tape (m)
ε_m	Eddy kinematic viscosity ($m^2\,s^{-1}$)
ν	kinematic viscosity ($m^2\,s^{-1}$)
ρ	fluid density ($kg\,m^{-3}$)
τ	shear stress (Pa)

Dimensionless groups

e_S^+	dimensionless equivalent sand grain roughness $(e_S u_*/\nu)$
f	Fanning friction factor $(2\tau_w/(\rho U_m^2))$
l^+	dimensionless mixing length (lu_*/ν)
Re	Reynolds number $(U_m D/\nu)$
r_0^+	dimensionless tube radius $(r_0 u_*/\nu)$
U^+	dimensionless axial velocity (U/u_*)
y^+	dimensionless distance from the wall (yu_*/ν)
β_*	$\beta/90$
η	dimensionless distance from the wall (y/r_0)
$\Delta\eta$	dimensionless shift $(\Delta y/r_0)$

Subscripts

a	axial
c	core region
D	buffer zone
H	hydraulic
i	inside diameter
m	mean value
max	maximum value
t	tangential
v	vortex
w	wall

the dimensionless twist ratio H/D_i and the dimensionless thickness δ/D_i of the tape [3]. The smaller the twist ratio the greater the heat transfer enhancement [5]. A lower bound for the enhancement effect corresponds to $H/D_i = \infty$ or a straight tape insert which partitions the tube into two semicircular segments.

It is well known that two or more of the existing techniques can be utilized simultaneously to produce an enhancement larger than that produced by only one technique. The combination of different techniques acting simultaneously is known as compound enhancement. Interactions between different enhancement methods contribute to greater values of the heat transfer coefficient compared to the sum of the corresponding values for the individual techniques used alone. The recent articles [6–9] report on an experimental investigation to see whether or not heat transfer can be enhanced by the multiplicative effect of a corrugated tube combined with a twisted tape insert. The geometrical characteristics of the corrugated tube and twisted tape insert are shown in Fig. 1. Despite of the fact that a comprehensive study was conducted on a variety of corrugated tubes combined with twisted tapes, a lack of sufficient knowledge about the flow mechanism does not permit the prediction of the friction factors and heat transfer coefficients by analytical methods.

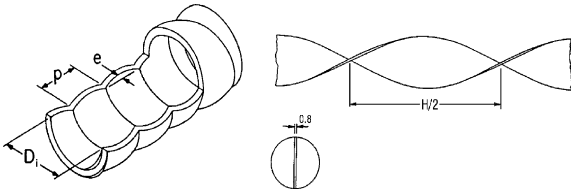

Fig. 1. Geometrical characteristics of a corrugated tube and twisted tape insert.

The purpose of this paper is to create a simple mathematical model to predict the heat transfer coefficients for the case of a fully developed single-phase turbulent flow in a corrugated tube combined with a twisted tape insert.

2. The mathematical model

The model refers to heat transfer for a fully developed one-dimensional turbulent pipe flow in a corrugated tube combined with a twisted tape insert. The results are obtained if the following assumptions hold:

(a) the fluid is single-phase, incompressible and its physical properties are constant;

(b) the transport processes are time independent;
(c) the turbulent flow is both hydrodynamically and thermally stabilized;
(d) the axial conduction and viscous dissipation in the fluid are neglected.

The physical model used in the friction factor analysis [10] also serves as a basis for the heat transfer predictions and the complexity of the results is a function of the boundary layer details and the Prandtl number effects considered. The total heat transfer in the absence of tape fin effects will therefore be due to the additive effects of the tube wall boundary layer flow and the energy interchange caused by vortex mixing. An investigation of Migai [11] revealed that the thermal resistance distribution of the fluid in the different parts of the boundary layer is quite ununiform and has a very strong Prandtl number dependence. For example, for $Re = 10^4$ and $Pr = 0.7$ the thermal resistances of the laminar sublayer, buffer zone and turbulent core are respectively 32.3%, 52.0% and 15% of the total thermal resistance; for $Re = 10^4$ and $Pr = 10.0$—these quantities are 74.6%, 22.0% and 3.4%, respectively. It is very remarkable that the bigger part of the total thermal resistance for $Pr = 0.7$ is distributed in the buffer zone and turbulent core instead of in the laminar sublayer. On the other hand, it is well known that when Re increases the thickness of the laminar sublayer gradually decreases and it has to be expected that the thermal resistance of the sublayer will be smaller than the pure axial flow due to the superposed vortex motion. When "wall roughness" and vortex fluid motion are combined this will cause additional decrease in the thickness of the laminar sublayer. From the above it follows that for gases ($Pr = 0.7$) the thermal resistance of the laminar sublayer can be neglected without any substantial error whereas for liquids ($Pr > 1$) it cannot be ignored and has to be taken into account. This idea has been very successfully implemented to predict the heat transfer coefficients for turbulent flow in a smooth pipe with a twisted tape insert [12]. Therefore, the model for the heat transfer process has to reflect both the effect of the presence of the "wall roughness" and twisted tape insert and the change in the thermal resistance of the viscous sublayer. To evaluate the simultaneous impact of the "wall roughness" and twisted tape insert on the total thermal resistance of the fluid one must take into account the increased wall heat flux due to the axial, tangential and vortex mixing tube flows

$$q_{\mathrm{tot}} = q_{\mathrm{w}} = q_{\mathrm{a}} + q_{\mathrm{t}} + q_{\mathrm{v}} = q_{\mathrm{a,t}} + q_{\mathrm{v}} \tag{1}$$

and

$$St = \frac{q_{\mathrm{w}}}{\rho c_p U_{\mathrm{m}}(T_{\mathrm{w}} - T_{\mathrm{m}})} = \frac{q_{\mathrm{a,t}} + q_{\mathrm{v}}}{\rho c_p U_{\mathrm{m}}(T_{\mathrm{w}} - T_{\mathrm{m}})} = St_{\mathrm{a,t}} + St_{\mathrm{v}}. \tag{2}$$

The heat transfer coefficients $St_{\mathrm{a,t}}$ and St_{v} can be described as follows:

(i) The heat transfer attributable to axial turbulent tube flow—$St_{\mathrm{a}} = Nu_{\mathrm{a}}/(Re_{\mathrm{H}} Pr)$. This contribution is obtainable through the evaluation of the thermal resistance of the axial turbulent tube flow. The latter can be decomposed into two components:

(a) the thermal resistance of the core region, $2e/D_{\mathrm{i}} < \eta \leqslant 1$, St_{c}^{-1},
(b) the thermal resistance of the fluid nearest to the wall and surrounding the roughness elements in the region $0 \leqslant \eta \leqslant 2e/D_{\mathrm{i}}$, including the thermal resistance of the viscous sublayer and buffer zone, St_{w}^{-1}.

Having this in mind one can describe the thermal resistance of the axial tube flow in the form of a Stanton number as

$$St_{\mathrm{a}}^{-1} = \frac{\rho c_p U_{\mathrm{m}}}{q_{\mathrm{a}}}(T_{\mathrm{w}} - T_{\mathrm{m}}) = St_{\mathrm{w}}^{-1} + St_{\mathrm{c}}^{-1}. \tag{3}$$

The thermal resistance of the turbulent core, St_{c}^{-1}, can be obtained through the value of the Lyon's integral [13] Nu_{c} for prescribed value of Re_{H} as

$$Nu_{\mathrm{c}}^{-1} = 2\int_0^1 \frac{\left(\int_{1-\eta}^{\eta}(1-\eta)U^+(\eta)\,\mathrm{d}\eta\right)^2}{(1-\eta)\left(1 + \frac{Pr}{Pr_{\mathrm{t}}}\frac{\varepsilon_{\mathrm{m}}}{\nu}\right)}\mathrm{d}\eta \tag{4}$$

where the distributions of $U^+(\eta)$ and $\varepsilon_{\mathrm{m}}/\nu(\eta)$ are already available. The turbulent Prandtl number Pr_{t} is defined [14] as

$$Pr_{\mathrm{t}} = 0.909\frac{B^+}{26}, \quad \eta = 0, \tag{5}$$

$$Pr_{\mathrm{t}} = 0.909\frac{1 - \exp(-\eta r_0^+/26)}{1 - \exp(-\eta r_0^+/B^+)}, \quad 0 < \eta \leqslant \eta_{\mathrm{w}}, \tag{6}$$

$$Pr_{\mathrm{t}} = 0.909, \quad \eta_{\mathrm{w}} < \eta \leqslant 1, \tag{7}$$

$$B^+ = Pr^{-0.5}\sum_1^5 C_k(\log_{10} Pr)^{k-1}, \quad 0.02 < Pr < 15, \tag{8}$$

where $C_1 = 34.96$, $C_2 = 28.79$, $C_3 = 33.95$, $C_4 = 6.33$, $C_5 = -1.186$.

The thermal resistance of the fluid nearest to the wall and surrounding the roughness elements, St_{w}^{-1}, is taken into account only for liquids, $Pr > 1$. One of the effects of the twisted tape insert and the "wall roughness" is the reduction of the thermal resistance of the flow nearest the wall, which gradually diminishes when Reynolds and Prandtl numbers increase. This resistance, denoted as ΔT_{S}^+, has been evaluated through integrating Eq. (20) for $\eta = \eta_{\mathrm{v,S}}$ and linear distribution for q/q_{w}. Thus

$$\Delta T_S^+ = T_w^+ - T_S^+ = \int_0^{\eta_{v,S}} \frac{(1-\eta)}{\frac{1}{r_0^+}\left(\frac{1}{Pr}+\frac{1}{Pr_t}\frac{\varepsilon_m}{\nu}\right)}\,d\eta, \quad (9)$$

where $r_0^+ = 0.5 Re_H (D_i/D_H)\sqrt{f/2}$. It has been assumed that $\eta_{v,S} \propto Pr^{-0.4}$ and it can be calculated as $\eta_{v,S} = (4\eta_D + \Delta\eta)Pr^{-0.4}$, but no smaller than $0.25e/D$. The Stanton number St_w^{-1} is calculated from

$$St_w^{-1} = (T_w^+ - T_S^+)\sqrt{2/f}. \quad (10)$$

When the corrugated tube acts alone (without a twisting tape insert) the wall layer thermal resistance St_w^{-1} depends essentially on the particular type of wall roughness and can be defined from [15]

$$St_w^{-1} = \frac{T_w^+ - T_e^+}{\sqrt{(f/2)}} = g(e^+, Pr)\sqrt{(2/f)} = St^{-1} - St_c^{-1}. \quad (11)$$

It is calculated as the difference between the total thermal resistance and the core thermal resistance. Since the function $g(e^+, Pr)$ is sensitive to the shape of the ridges or ribs it has been derived using experimental data for f and St only from the corrugated tubes used in the experimental program [6–9]. This function could be related to the following characteristic geometrical parameters of the tubes to obtain a simple power law correlation in the form

$$g(e^+, Pr)Pr^{-0.6} = 5.334 Re^{0.089}(e/D_i)^{-0.113}(p/e)^{-0.264}\beta_*^{-0.180}, \quad p/e \geqslant 9.0, \quad (12a)$$

and

$$g(e^+, Pr)Pr^{-0.6} = 299.6 Re^{0.131}(e/D_i)^{0.009}(p/e)^{-2.056}\beta_*^{2.655}, \quad p/e = 7.0\text{–}9.0. \quad (12b)$$

To verify the validity of the g-function, Eq. (12), in the case of a corrugated tube acting alone, heat transfer coefficients (St) have been calculated from Eqs. (3)–(8), (11) and (12) and compared with 114 experimental points [6–9]. Ninety three points (81.6%) showed a relative difference of less than ±10%; for 18 points (15.8%) this difference is ±(10–15)% and for the remaining only three points the difference is greater than ±15%.

It has been assumed that when corrugated tubes are combined with twisted tape inserts the thermal resistance of the wall layer calculated from Eq. (11) should decrease. In this regard, the thermal resistance calculated from Eq. (10) has been restricted not to exceed that one calculated from Eq. (11).

(ii) The heat transfer attributable to axial and tangential tube wall flows—$St_{a,t}$. To evaluate the contribution due to the axial and tangential tube wall flows a Reynolds analogy is used [2] assuming that an effective shear stress $\tau_{a,t}$ can be defined which is dependant on the total velocity vector at the edge of the buffer zone

$$\frac{\tau_{a,t}}{\tau_a} = \frac{V_S}{U_m} = \left(1 + \frac{(1-\eta_D)^2\pi^2}{(H/D_i)^2}\right)^{0.5} \quad (13)$$

and the heat transfer will increase in the same proportion

$$\frac{q_{a,t}}{q_a} = \frac{St_{a,t}}{St_a} = \left(1 + \frac{(1-\eta_D)^2\pi^2}{(H/D_i)^2}\right)^{0.5}. \quad (14)$$

(iii) The heat transfer attributable to the vortex mixing flow—St_v. As in the friction factor analysis [10] it is assumed that the principal boundary layer contributions to the vortex mixing arise from the viscous sublayer and the buffer zone but the energy transport is increased additionally due to the presence of the surface roughness at a distance of $\eta_v > \eta_D$. The heat flux convected from the boundary layer into the main stream [2] is

$$d\dot{Q}_v = c_p\, d\dot{m}(T - T_S),$$

for each half of the tube, where $d\dot{m} = \rho V_t\, dr\, dx$ and

$$dq_v = \frac{d\dot{Q}_v}{\pi r_0\, dx} = \frac{\rho c_p V_t (T - T_S)}{\pi}\, d\eta. \quad (15)$$

Substituting V_t from Eqs. (8) and (9) [10],

$$V_t = \frac{(1-\eta_D)}{\eta_D}\frac{\pi U_m}{(H/D_i)}\eta, \quad 0 \leqslant \eta \leqslant \eta_D,$$

$$V_t = \frac{\pi U_m}{(H/D_i)}(1-\eta), \quad \eta_D \leqslant \eta \leqslant \eta_v,$$

and integrating Eq. (15) in the limits $0 \leqslant \eta \leqslant \eta_v$

$$q_v = \frac{\rho c_p}{\pi}\int_0^{\eta_v} V_t(T - T_S)\, d\eta = \frac{\rho c_p}{\pi}\left(\int_0^{\eta_D} V_t(T - T_S)\, d\eta + \int_{\eta_D}^{\eta_v} V_t(T - T_S)\, d\eta\right), \quad (16)$$

where $\eta_D = \frac{30\sqrt{2}}{Re_H\sqrt{f}(D_i/D_H)}$. It is assumed that the distance η_v to be $1.5\eta_D$ but no smaller than $0.5e/D_i$; $\eta_v = 1.5\eta_D \geqslant 0.5e/D_i$. Introducing the Stanton number,

$$St_v = \frac{q_v}{\rho c_p U_m (T_w - T_m)} = \frac{(1-\eta_D)}{\eta_D(H/D_i)}\int_0^{\eta_D}\frac{T - T_S}{T_w - T_m}\eta\, d\eta + \frac{1}{(H/D_i)}\int_{\eta_D}^{\eta_v}\frac{T - T_S}{T_w - T_m}(1-\eta)\, d\eta$$

or

$$St_v = \frac{(1-\eta_D)}{\eta_D(H/D_i)}\int_0^{\eta_D}\frac{T^+ - T_S^+}{T_w^+ - T_m^+}\eta\, d\eta + \frac{1}{(H/D_i)}\int_{\eta_D}^{\eta_v}\frac{T^+ - T_S^+}{T_w^+ - T_m^+}(1-\eta)\, d\eta, \quad (17)$$

where

$$T_w^+ - T_m^+ = \frac{\sqrt{f/2}}{St};$$
$$T^+ - T_S^+ = (T_w^+ - T_S^+) - (T_w^+ - T^+) = \Delta T_S^+ - \Delta T^+.$$

The temperature differences ΔT_S and ΔT^+ can be obtained from integration of the usual heat flux relation

$$q = -(a + \varepsilon_H)\rho c_p \frac{dT}{dy}, \tag{18}$$

in dimensionless form

$$\frac{q}{q_w} = -\frac{\left(1 + \frac{Pr}{Pr_t}\frac{\varepsilon_m}{\nu}\right)}{r_0^+ Pr}\frac{\partial T^+}{\partial \eta}. \tag{19}$$

Thus,

$$\Delta T_S^+ = T_w^+ - T_S^+ = \int_0^{\eta_v} \frac{q/q_w}{\frac{1}{r_0^+}\left(\frac{1}{Pr} + \frac{1}{Pr_t}\frac{\varepsilon_m}{\nu}\right)} d\eta, \tag{20}$$

$$\Delta T^+ = \int_0^{\eta} \frac{q/q_w}{\frac{1}{r_0^+}\left(\frac{1}{Pr} + \frac{1}{Pr_t}\frac{\varepsilon_m}{\nu}\right)} d\eta. \tag{21}$$

Using the linear distribution for q/q_w, Eq. (17) yields

$$\begin{aligned} St_v = {} & \frac{(1-\eta_D)St}{\eta_D (H/D_i)\sqrt{f/2}}\left(\frac{\eta_D^2}{2}\int_0^{\eta_v} \frac{(1-\eta)}{\frac{1}{r_0^+}\left(\frac{1}{Pr} + \frac{1}{Pr_t}\frac{\varepsilon_m}{\nu}\right)} d\eta \right. \\ & \left. - \int_0^{\eta_D}\left(\int_0^{\eta_v} \frac{(1-\eta)}{\frac{1}{r_0^+}\left(\frac{1}{Pr} + \frac{1}{Pr_t}\frac{\varepsilon_m}{\nu}\right)} d\eta\right)\eta\, d\eta\right) \\ & + \frac{St}{(H/D_i)\sqrt{f/2}}\left((\eta_v - \eta_D)\left(1 - \frac{1}{2}(\eta_v - \eta_D)\right)\right. \\ & \times \int_0^{\eta_v} \frac{(1-\eta)}{\frac{1}{r_0^+}\left(\frac{1}{Pr} + \frac{1}{Pr_t}\frac{\varepsilon_m}{\nu}\right)} d\eta \\ & \left. - \int_{\eta_D}^{\eta_v}\left(\int_0^{\eta} \frac{(1-\eta)}{\frac{1}{r_0^+}\left(\frac{1}{Pr} + \frac{1}{Pr_t}\frac{\varepsilon_m}{\nu}\right)} d\eta\right)(1-\eta) d\eta\right). \end{aligned} \tag{22}$$

The model discussed here comprises the following cases concerning the calculation of the heat transfer coefficient for a fully developed turbulent flow in a pipe:

(a) $\Delta\eta = 0$; $H/D_i = 0$ and $St_w^{-1} = 0$—the model calculates the friction factor and heat transfer coefficient for a smooth pipe [16];
(b) $\Delta\eta > 0$, $H/D_i = 0$ and $St_w^{-1} > 0$—the model calculates the friction factor and heat transfer coefficient for a corrugated pipe [15];
(c) $\Delta\eta = 0, H/D_i > 0$ and $St_w^{-1} > 0$—the model calculates the friction factor and heat transfer coefficient for a smooth pipe combined with a twisted tape insert [12];
(d) $\Delta\eta > 0$, $H/D_i > 0$ and $St_w^{-1} > 0$—the model calculates the friction factor and heat transfer coefficient for a corrugated tube combined with a twisted tape insert.

3. Results and discussion

The heat transfer coefficients (transformed as Stanton numbers) have been calculated using Eqs. (2)–(22) and compared with 544 experimental points obtained from 57 corrugated tubes combined with twisted tape inserts. The values of the geometrical parameters of the corrugated tubes are presented in Table 1. Two hundred sixty-eight points (49.3%) have a relative difference of less than ±10%, for 170 points this difference is ±10–15%, and for the remaining 106 points the difference is ±15–20%. The numerical results for the heat transfer coefficients (transformed as Nusselt numbers) together with the experimental data of the tubes studied (corrugated tubes combined with twisted tape inserts) are presented in Figs. 2–13. Taking into account the experimental error in the measurements, this agreement should be considered as fairly acceptable. Because of the lack of other experimental data of this kind (for corrugated tubes with twisted tape inserts) an attempt to verify the model has been made with the study of Bergles

Table 1
Values of the characteristic parameters of the corrugated tubes

Tube	D_i (mm)	e (mm)	p (mm)	β (°)	e/D_i	p/e	β_*
3010	13.90	0.312	5.76	82.4	0.0224	18.46	0.916
3020	12.44	0.515	4.48	83.4	0.0414	8.70	0.927
3040	13.39	0.497	5.77	82.2	0.0371	11.61	0.913
3050	13.15	0.593	5.06	83.0	0.0451	8.53	0.922
3070	13.66	0.622	8.12	79.3	0.0456	13.05	0.881
4020	13.53	0.507	4.55	72.2	0.0375	8.97	0.802
4030	13.73	0.781	5.82	68.0	0.0569	7.45	0.755
4040	13.68	0.557	5.97	67.4	0.0407	10.73	0.749
4050	13.38	0.581	5.08	70.1	0.0434	8.74	0.779
2010	13.68	0.315	6.67	90.0	0.0230	21.17	1.000
2040	13.65	0.440	6.01	90.0	0.0322	13.66	1.000
2070	13.59	0.464	8.55	90.0	0.0341	18.43	1.000

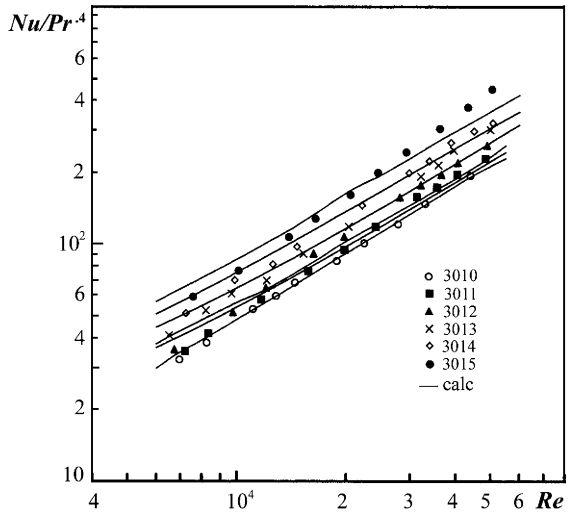

Fig. 2. Nusselt number vs. Reynolds number. Comparison between computed and experimental results ($3010 - H/D_i = 0$; $3011 - H/D_i = 15.11$; $3012 - H/D_i = 12.09$; $3013 - H/D_i = 7.63$; $3014 - H/D_i = 5.76$; $3015 - H/D_i = 4.75$).

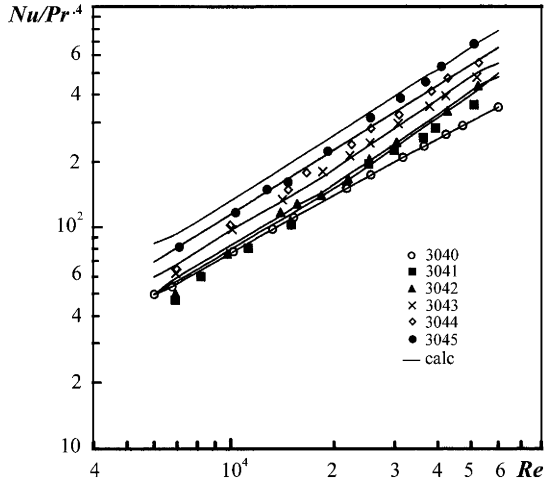

Fig. 4. Nusselt number vs. Reynolds number. Comparison between computed and experimental results ($3040 - H/D_i = 0$; $3041 - H/D_i = 15.68$; $3042 - H/D_i = 12.54$; $3043 - H/D_i = 7.91$; $3044 - H/D_i = 5.97$; $3045 - H/D_i = 4.85$).

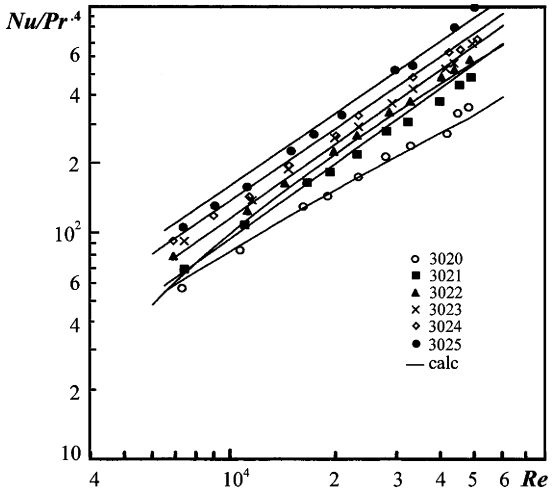

Fig. 3. Nusselt number vs. Reynolds number. Comparison between computed and experimental results ($3020 - H/D_i = 0$; $3021 - H/D_i = 16.88$; $3022 - H/D_i = 13.50$; $3023 - H/D_i = 8.52$; $3024 - H/D_i = 6.43$; $3025 - H/D_i = 5.23$).

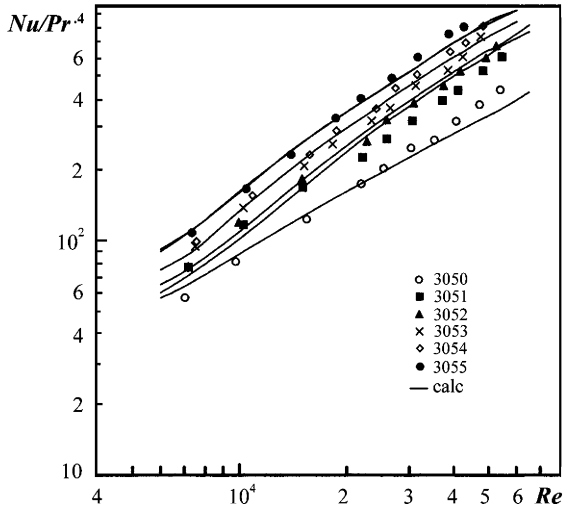

Fig. 5. Nusselt number vs. Reynolds number. Comparison between computed and experimental results ($3050 - H/D_i = 0$; $3051 - H/D_i = 15.97$; $3052 - H/D_i = 12.77$; $3053 - H/D_i = 8.06$; $3054 - H/D_i = 6.08$; $3055 - H/D_i = 4.94$).

et al. [17] where heat transfer coefficients for straight and swirl flow in rough tubes with twisted tape inserts were reported, Fig. 14. The authors suggested an equivalent sand grain roughness of $e_S/D_i = 0.005$–0.015. Giving different values of e_S/D_i for different Reynolds numbers the friction factors have been calculated through the model discussed in [10]. Since the roughness was suggested as one-dimensional (equivalent sand grain roughness) the model presented in [18] has been used to predict the heat transfer coefficient in a rough tube (without twisted tape insert). In this case, the g-function has been determined through the experimental data of [17] in the form

$$g(e_S^+, Pr) = 5.9668(e_S^+)^{0.246} Pr^{0.6}. \quad (23)$$

The calculated values of the heat transfer coefficient for the rough tube acting alone are very close to the experimental data (relative difference of less than ±5%)

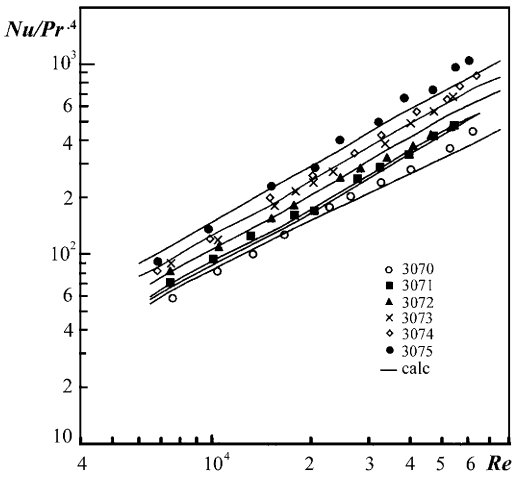

Fig. 6. Nusselt number vs. Reynolds number. Comparison between computed and experimental results ($3070 - H/D_i = 0$; $3071 - H/D_i = 15.38$; $3072 - H/D_i = 12.31$; $3073 - H/D_i = 7.77$; $3074 - H/D_i = 5.86$; $3075 - H/D_i = 4.76$).

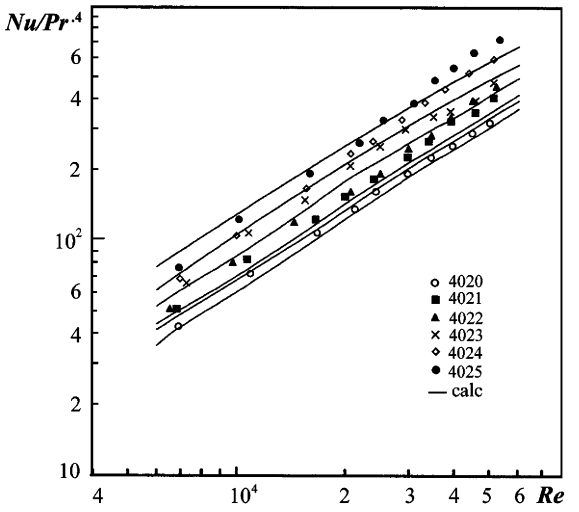

Fig. 7. Nusselt number vs. Reynolds number. Comparison between computed and experimental results ($4020 - H/D_i = 0$; $4021 - H/D_i = 15.52$; $4022 - H/D_i = 12.42$; $4023 - H/D_i = 7.83$; $4024 - H/D_i = 5.91$; $4025 - H/D_i = 4.80$).

whereas for the combination of a rough tube of this kind and a twisted tape insert the calculated values are (20–25)% higher compared to the experimental results [17], Fig. 14.

4. Conclusions

The results of the present study can be summarized as follows:

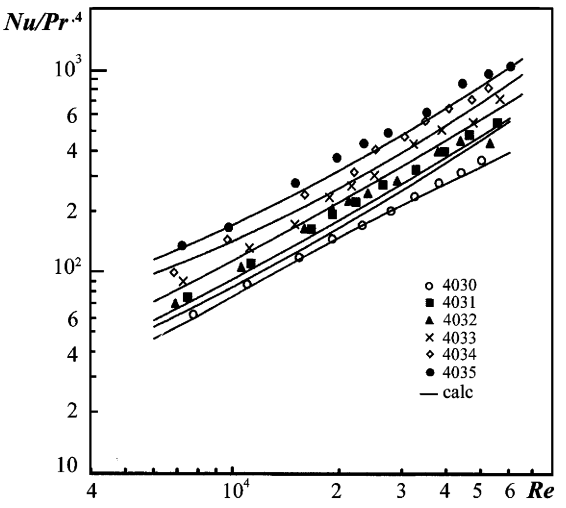

Fig. 8. Nusselt number vs. Reynolds number. Comparison between computed and experimental results ($4030 - H/D_i = 0$; $4031 - H/D_i = 15.30$; $4032 - H/D_i = 12.24$; $4033 - H/D_i = 7.72$; $4034 - H/D_i = 5.83$; $4035 - H/D_i = 4.73$).

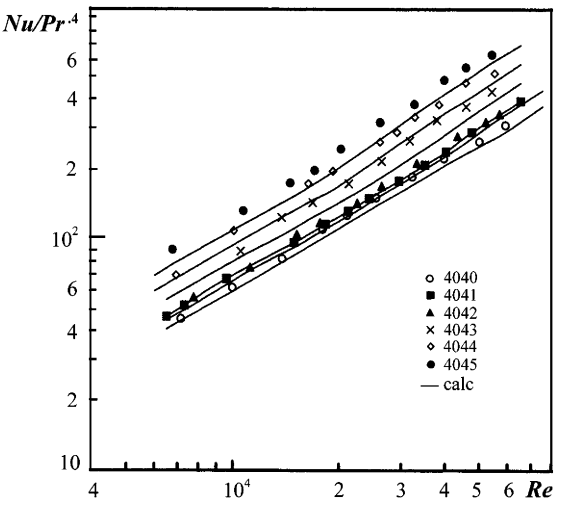

Fig. 9. Nusselt number vs. Reynolds number. Comparison between computed and experimental results ($4040 - H/D_i = 0$; $4041 - H/D_i = 15.35$; $4042 - H/D_i = 12.28$; $4043 - H/D_i = 7.75$; $4044 - H/D_i = 5.85$; $4045 - H/D_i = 4.75$).

(1) A simple mathematical model has been created to predict the heat transfer coefficients for the case of a fully developed turbulent flow in a spirally corrugated tube combined with a twisted tape insert which is an extension and modification of the idea of Smithberg and Landis to predict heat transfer coefficients for turbulent flow in a smooth tube with a twisted tape insert.

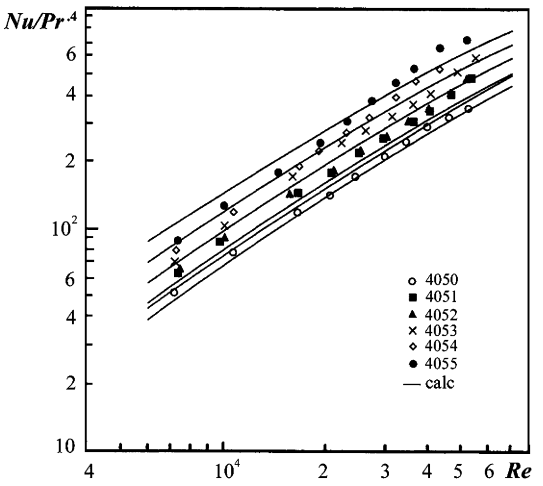

Fig. 10. Nusselt number vs. Reynolds number. Comparison between computed and experimental results ($4050 - H/D_i = 0$; $4051 - H/D_i = 15.69$; $4052 - H/D_i = 12.55$; $4053 - H/D_i = 7.92$; $4054 - H/D_i = 5.98$; $4055 - H/D_i = 4.86$).

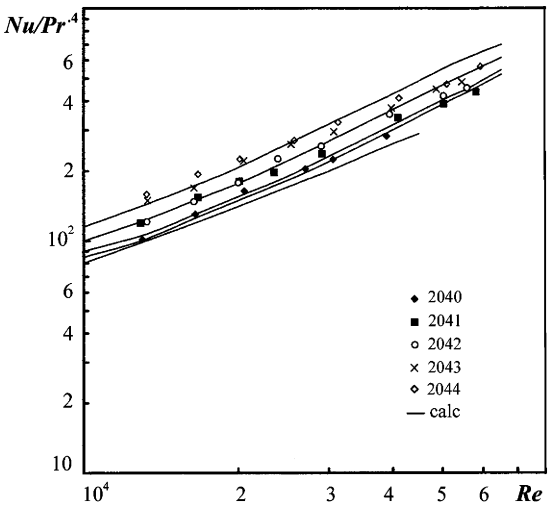

Fig. 12. Nusselt number vs. Reynolds number. Comparison between computed and experimental results ($2040 - H/D_i = 0$; $2041 - H/D_i = 15.38$; $2042 - H/D_i = 12.30$; $2043 - H/D_i = 7.76$; $2044 - H/D_i = 5.86$).

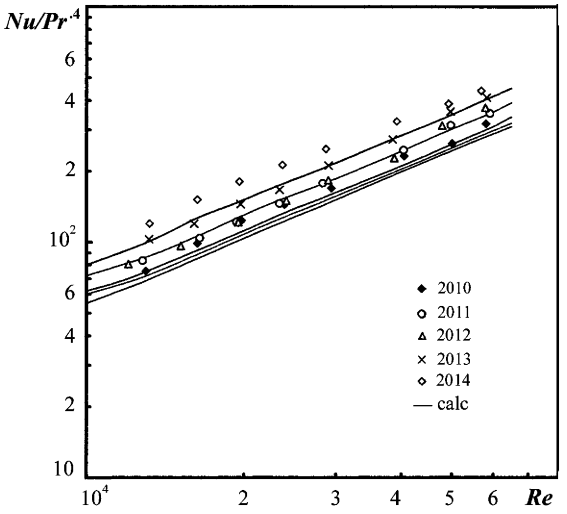

Fig. 11. Nusselt number vs. Reynolds number. Comparison between computed and experimental results ($2010 - H/D_i = 0$; $2011 - H/D_i = 15.35$; $2012 - H/D_i = 12.28$; $2013 - H/D_i = 7.75$; $2014 - H/D_i = 5.85$).

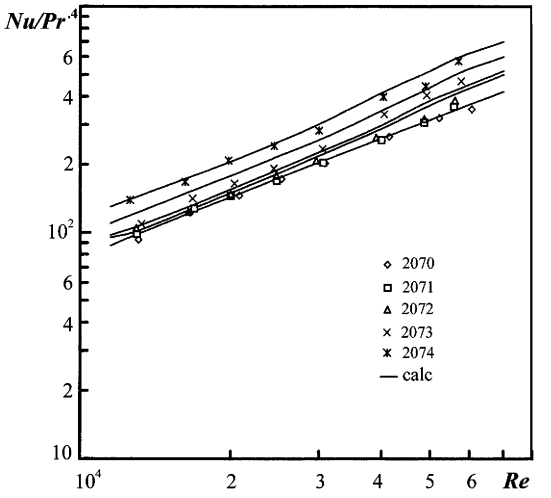

Fig. 13. Nusselt number vs. Reynolds number. Comparison between computed and experimental results ($2070 - H/D_i = 0$; $2071 - H/D_i = 15.45$; $2072 - H/D_i = 12.36$; $2073 - H/D_i = 7.80$; $2074 - H/D_i = 5.89$).

(2) The model reflects the influence of the "wall roughness" and the twisted tape on the thermal resistances of the helicoidal core flow, twisting boundary layer flow and the viscous sublayer near the wall.
(3) The calculated heat transfer coefficients have been compared with 544 experimental points obtained from 57 tubes tested. Four hundred thirty-eight points (80.5%) have a relative difference of less than ±15% and for the remaining 106 points this difference is ±(15–20)%. To verify the validity of the model for another type "wall roughness" the calculated heat transfer coefficients for turbulent flow in rough tubes (sand grain roughness) with twisted tape inserts have been compared with the experimental data of Bergles et al. [17]. The agreement between predicted and experimental data is fairly good.
(4) The model comprises the possibilities to predict the heat transfer coefficients for the cases of a turbulent

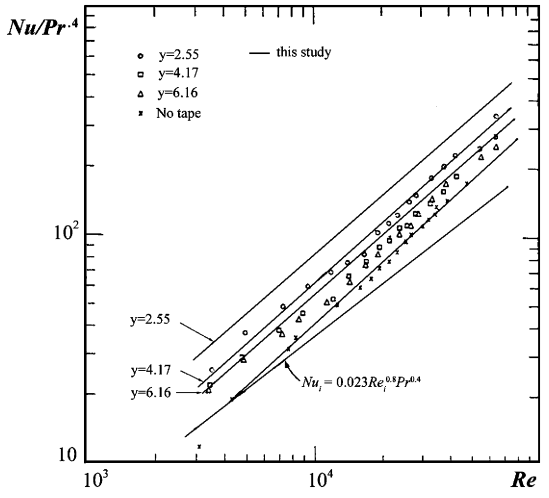

Fig. 14. Nusselt number vs. Reynolds number. Comparison between computed and experimental results of [5] ($y = 0.5H/D_i$).

flow in a smooth pipe; a smooth pipe with a twisted tape insert; a corrugated tube and a corrugated tube combined with a twisted tape insert.

References

[1] A.E. Bergles, Survey and evaluation of techniques to augment convective heat and mass transfer, Prog. Heat Mass Transfer 1 (1969) 331–424.

[2] E. Smithberg, F. Landis, Friction and forced convection heat transfer characteristics in tubes with twisted tape swirl generators, Trans. ASME, J. Heat Transfer 86 (1964) 39–49.

[3] R.M. Manglik, A.E. Bergles, Heat transfer enhancement and pressure drop in viscous liquid flows in isothermal tubes with twisted-tape inserts, Warme. Stoffubertrag. 27 (1992) 249–257.

[4] R.M. Manglik, A.E. Bergles, Heat transfer and pressure drop correlations for twisted-tape inserts in isothermal tubes. Part II. Transition and turbulent flows, Trans. ASME, J. Heat Transfer 115 (1993) 890–896.

[5] A.E. Bergles, Techniques to augment heat transfer, in: Handbook of Heat Transfer Applications, vol. 3-1, McGraw-Hill, New York, 1985, pp. 3–80 (Chapter 3).

[6] V.D. Zimparov, Enhancement of heat transfer by a combination of three-start spirally corrugated tubes with a twisted tape insert, Int. J. Heat Mass Transfer 44 (2001) 551–574.

[7] V.D. Zimparov, Enhancement of heat transfer by a combination of a single-start spirally corrugated tubes with a twisted tape, Exp. Thermal Fluid Sci. 25 (2002) 535–546.

[8] V.D. Zimparov, V.M. Petkov, Compound heat transfer augmentation by a combination of spirally corrugated tubes with a twisted tape, in: Proceedings of 1st International Conference of Heat Transfer, Fluid Mechanics and Thermodynamics, Kruger National Park, South Africa, vol. 1, 2002, pp. 547–552.

[9] V.D. Zimparov, V.M. Petkov, Compound heat transfer enhancement by a combination of spirally corrugated tubes with a twisted tape, in: Proceedings of 12th International Heat Transfer Conference, Grenoble, France, vol. 4, 2002, pp. 53–158.

[10] V.D. Zimparov, Prediction of friction factors and heat transfer coefficients for turbulent flows in corrugated tubes combined with twisted tape inserts. Part 1: Friction factors, Int. J. Heat Mass Transfer, in press.

[11] V.K. Migai, Exchanger Performance Improvement, Energia, Leningrad, 1980 (in Russian).

[12] V.D. Zimparov, A mathematical model to predict heat transfer coefficients for turbulent intube flow with twisted tape inserts, J. TU-Gabrovo 27 (2003) 9–14.

[13] R.N. Lyon, Liquid metal heat transfer, Chem. Eng. Prog. 47 (1951) 75–79.

[14] T. Cebeci, A.M.O. Smith, Analysis of Turbulent Boundary Layers, Academic Press, New York, 1974.

[15] N.L. Vulchanov, V.D. Zimparov, L.B. Delov, Heat transfer and friction characteristics of spirally corrugated tubes for power plant condensers—2. A mixing length model for predicting fluid friction and heat transfer, Int. J. Heat Mass Transfer 34 (9) (1991) 2199–2206.

[16] M.D. Mikhailov, N.L. Vulchanov, V.D. Zimparov, Computation of stabilized turbulent flow and heat transfer in circular smooth pipes for moderate Prandtl numbers. Part 2. The limiting heat transfer coefficients, Bulg. Acad. Sci., Theor. Appl. Mech. XVI (4) (1985) 49–54.

[17] A.E. Bergles, R.A. Lee, B.B. Mikic, Heat transfer in rough tubes with twisted tape swirl flow, Trans. ASME, J. Heat Transfer 91 (1969) 443–445.

[18] N.L. Vulchanov, V.D. Zimparov, Stabilized turbulent fluid friction and heat transfer in circular tubes with internal sand type roughness at moderate Prandtl numbers, Int. J. Heat Mass Transfer 32 (1) (1989) 29–34.